

NUMERICAL SIMULATION OF FLOW PAST A CIRCULAR CYLINDER IN ELLIPTIC ORBIT AT LOW REYNOLDS NUMBER

Eric Didier^{1,2}

¹ MARETEC, IST, Lisbon, Portugal

² FCT-UNL, Lisbon, Portugal

ABSTRACT

Two-dimensional fluid flow around an oscillating circular cylinder in elliptic motion at Reynolds number 300 is investigated numerically for different oscillation frequency and orbit ellipticity. An original fully coupled numerical method is used for simulating the non-stationary flow. Occurrence of lock-in, characterized by a large jump of fundamental quantity values, is observed and lock-in regions are determined. Under lock-in conditions, mean lift coefficient pre-sents negative and positive values. The variations of fluctuating lift and mean drag coefficients show different behavior and slope of curves change with ellipticity. Curve of fluctuating drag coefficient widely changes and maximum value is not reach for the highest lock-in frequency, like the other fundamental quantities, but for a frequency all the more small since the ellipticity is large.

1. INTRODUCTION

Study of flow past a circular cylinder is of special interest for basic understanding of the aerodynamics of aeroelastic phenomena. Despite the simplicity of geometry the flow around a cylinder is very complicated and of particular importance, since it may induce unsteady forces on structures associated with vortex shedding. Unsteady forces acting in both directions, in-line and transversal, represented by drag and lift coefficients respectively, can induce structure vibrations. Bodies oscillate in response to these forces, possibly in linear or orbital motion. In such cases the vortex shedding properties will change resulting in quite different lift and drag periodic fluctuations in time.

Most of the research efforts in the past have been concentrated on cross-flow oscillations since time-varying component of the lift force is usually an order of magnitude larger than that corresponding to the drag force. Cross-flow oscillating cylinder in uniform flow has been fairly widely researched, Williamson and Roshko (1988), Meneghini and Bearman (1995), Mittal and Kumar (1999), as have

in-line oscillating cylinder in uniform flow, Griffin and Ramberg (1975), Nobari and Naderan (2006), Al-Mdallal et al. (2007), or oscillatory flow, Bearman et al. (1985). A cylinder subjected to forced oscillation exhibits the phenomenon of lock-in: the vortex-shedding frequency of the oscillating cylinder changes to the frequency of cylinder vibrations, Koopmann (1967).

As already mentioned, the cylinder oscillations are predominantly in transversal direction, but in the majority of situations the cylinder follows a closed elliptic orbit, combination of in-line and transverse oscillations. However, there is relatively little investigation carried out for a cylinder in circular or elliptic motion. Among others, Chen et al. (1995) investigated numerically the orbital flow around a stationary cylinder; Williamson et al. (1998) studied experimentally a cylinder forced to follow an elliptic orbit; Stansby and Rainey (2001) carried out numerical investigation of the flow around a circular cylinder in circular motion in a current. Lewis (2006) investigated the orbital motion of a circular cylinder in a uniform flow using a vortex cloud flow modeling and compared its results with Baranyi (2004). Baranyi (2004) (2008) studied the flow around an orbiting cylinder at different ellipticity values from in-line to circular motion, employing a grid-based Eulerian type method for solving the two-dimensional Navier-Stokes equations. Abrupt jumps were found in the time-mean and root-mean-square (*rms*) values of the force coefficients caused by a critical change in the vortex structure.

The present study deals with an elliptic motion of a circular cylinder in a uniform flow at Reynolds number 300. Previously, Didier and Borges (2007) investigated the uniform flow around a circular cylinder in forced transverse, in-line and circular oscillation. Lock-in phenomenon is identified in all three cases. For circular orbit, the authors identified that slope variation of mean drag and fluctuating lift coefficients, under lock-in condition, has modified comparing with that obtained for transverse oscillation, indicating that this alteration is due to the longitudinal component of the motion. In the

present study, computations are carried out for various elliptic orbits. Ellipticity is varied from 0.0, a pure cross-flow oscillation, through a circular orbit, for ellipticity equal to 1.0. Oscillation frequency is varied over a broad range around the natural vortex-shedding frequency. The flow field changes significantly with oscillation frequency and orbit ellipticity and manifests in the forces experimented by the cylinder and the Strouhal number.

Computational investigations are performed considering an unsteady two-dimensional flow for an incompressible viscous fluid. Numerical simulations are carried out using an implicit second order fully coupled resolution method developed by the author (see Didier and Borges (2003)).

2. NUMERICAL METHOD

The numerical code FullCReM solves the unsteady, incompressible, two-dimensional Navier-Stokes equations, without any transformation of the continuity equation, Didier (2008). In the precedent version of the code, a pressure equation has been reconstructed, Didier and Borges (2003). This new approach is an alternative to classical segregated and coupled methods.

A finite volume method with collocated cell-centered unknowns is used to discretize the equations for structured or/and unstructured grids. Time-dependent solution of these equations requires using an implicit time-integration scheme: momentum equations are integrated with a three-level second order time scheme. The spatial discretization schemes are implicit too. Diffusion terms are approximated by second-order central-differences scheme. Newton linearization is applied to the convective terms and velocities are approximated by the deferred correction method, using UDS (first-order) and WACEB (third-order) schemes for the implicit and explicit part. Pressure at the midpoint face of the control volume is approximated by a second-order linear interpolation. For non-orthogonal grids, discrete schemes required corrections to estimate velocity and pressure to the face midpoint of the control volume. These explicit corrections, added to the source terms, are assumed to be small compared to the implicit part of the schemes.

The discretized continuity and momentum equations are solved simultaneously using the iterative algorithm Bi-CGSTAB- ω with an incomplete LU pre-conditioning. The present resolution method does not require any dual-time scheme like in the artificial compressibility or pressure correction methods, or any relaxation parameters. Whereas segregated methods lead to a sequential resolution of discrete equations, the fully coupled resolution method solves only one linear

system in velocity-pressure and allows reducing the number of non-linear iterations needed to converge. For details of numerical method, see Didier and Borges (2003) (2007), Didier (2008).

Figure 1 show the computational domain used to the present simulations. A grid refinement study made revealed that an O-grid with 200 and 180 nodes respectively in angular and radial direction, with a first grid-point near to the wall situated at $5.10^{-4}D$ is well adapted to the simulation of flow at Reynolds number $Re=300$. D is the cylinder diameter. A radius equal to $50D$ ensures that external boundary effects are sufficiently minimized. The non-dimensional time step is equal to 5.10^{-3} . The flow over the cylinder at $Re=300$ is considered laminar.

A no-slip condition is applied to the cylinder wall and free-stream velocity is imposed at the external boundary. The motion of the centre of the cylinder is specified as follows:

$$u_{o1}(t)=u_{e1} \cos(2 \omega f_{e1} t) \quad (1)$$

$$u_{o2}(t)=u_{e2} \sin(2 \omega f_{e2} t) \quad (2)$$

where u_{e1} , u_{e2} and f_{e1} , f_{e2} are the non-dimensional amplitude velocity and frequency of cylinder motion in longitudinal and transversal direction.

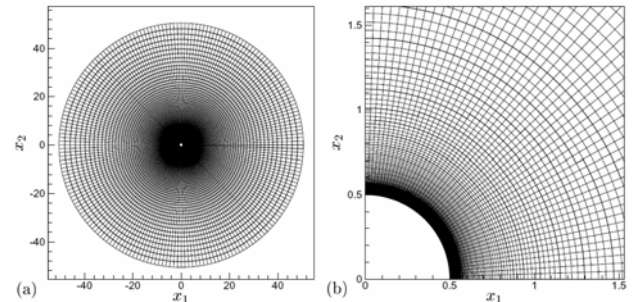


Figure 1: *Computational domain.*

The 2-D numerical code developed by the author has been extensively tested against experimental and computational results for fixed and oscillating cylinders and good agreement has been found, as can be seen in Didier and Borges (2003) (2005) (2007), Didier (2007) (2008), Baranyi (2008).

3. COMPUTATIONAL RESULTS

A goal of this work is to achieve a deeper understanding of the mechanisms that are involved in the alteration of the forces acting on a circular cylinder in elliptic orbit in uniform flow. With the aid of numerical simulations, mean and fluctuating drag and lift coefficients, and Strouhal number are calculated and presented.

Frequencies in longitudinal and transversal

direction are the same, $f_e = f_{e1} = f_{e2}$, and are in phase. Velocity amplitude in the transversal direction, u_{e2} , is equal to 10% of the free-stream velocity, U_o . Velocity amplitude in the longitudinal direction varies from 0 to 10% of the free-stream velocity in increment of 2%. Thus the cylinder describes a pure cross-flow motion, when $u_{e1}=0.0$, a circular orbit, when $u_{e1}=0.1U_o$, and an elliptic motion for other values of u_{e1} . Ellipticity, E , is defined as the ratio between the velocity amplitudes of the motion: $E = u_{e1} / u_{e2}$.

The data related to the stationary cylinder, Didier and Borges (2007), are shown in the figures by a dashed line and are defined as natural or reference values. The mean drag and lift coefficients are 1.352 and 0.0 respectively. The *rms* drag and lift are equal to 5.3×10^{-2} and 0.62 respectively. The Strouhal number is equal to 0.214.

Figure 2 shows Strouhal number variations with frequency and ellipticity. The Strouhal number is defined considering the predominant frequency in the spectrum, obtained by a Discrete Fourier Transform. Lock-in band is identified by the linearity relationship between frequency oscillation and Strouhal number. Figure 3 presents where lock-in occurs, i.e. when there is only one significantly dominant frequency. Figure 4 shows spectrum for $u_{e1}=0.08$ and $u_{e2}=0.10$ for the oscillation frequency range from 0.1950 to 0.2210. As can be seen, lock-in occurs between oscillation frequencies equal to 0.1975 and 0.2140. Before and after these frequencies, power spectrum presents two dominant frequencies: the oscillation frequency and the shedding frequency and eventual combination of these two frequencies.

The shedding frequency is globally smaller than the reference value for a fixe cylinder, $f_o=0.214$, except when lock-in occurs for frequencies higher than f_o . The lock-in bandwidth is all the more reduced since the ellipticity is large. For ellipticity equal to 0.8 and 1.0, the inferior and superior frequency limits, where lock-in occurs, are significantly reduced, compared to pure cross-flow oscillation. The superior limit moves near the natural vortex shedding frequency f_o . In all cases, minimum value of Strouhal number is obtained for the lowest lock-in frequency and the maximum for the highest lock-in frequency.

Figures 5 and 6 show the mean and *rms* lift coefficients versus the oscillation frequency. Figures 7 and 8 present the mean and *rms* drag coefficients.

It can be observed from all figures that as has been reported by various authors, the cylinder motion alters the flow field significantly. This effect manifests in the aerodynamic forces experienced by

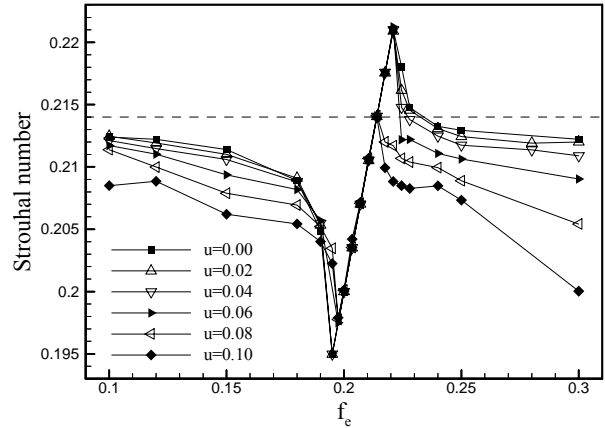


Figure 2: *St* versus the oscillation frequency.

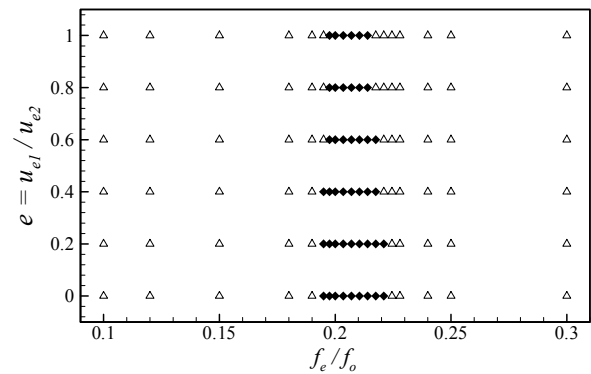


Figure 3: Simulation points for elliptic cylinder motion versus oscillation frequency: lock-in does not occur (Δ) and lock-in occurs (\blacklozenge).

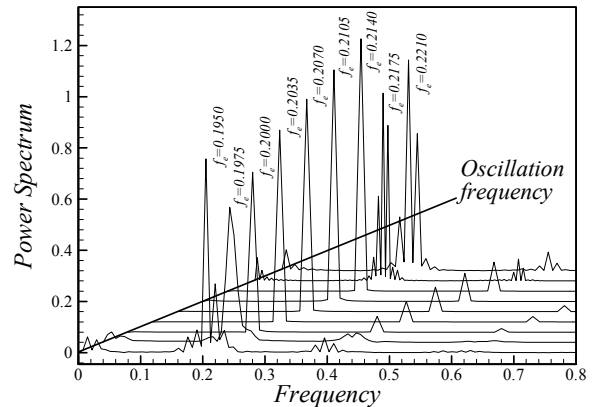


Figure 4: Power spectrum of fluctuating lift for orbit ellipticity $E=0.8$ and oscillation frequency between 0.1950 and 0.2210.

the cylinder and the Strouhal number.

Figures 5 and 6 show the mean and *rms* lift coefficients. If the mean C_L is zero for cross-flow it is not the case for elliptic and circular oscillation.

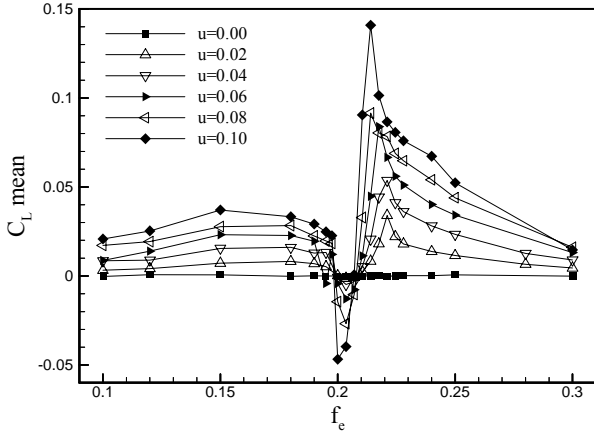


Figure 5: Mean lift coefficient versus oscillation frequency.

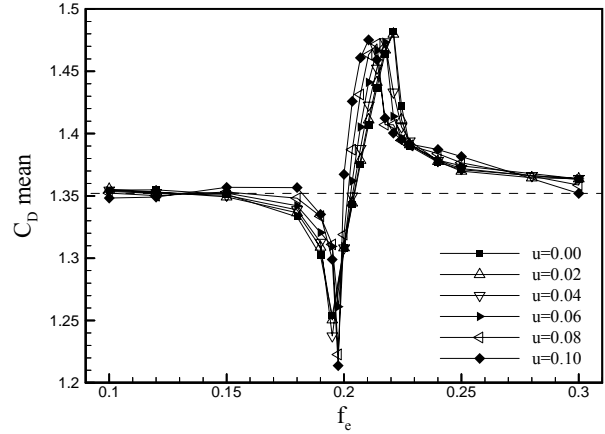


Figure 7: Mean drag coefficient versus oscillation frequency.

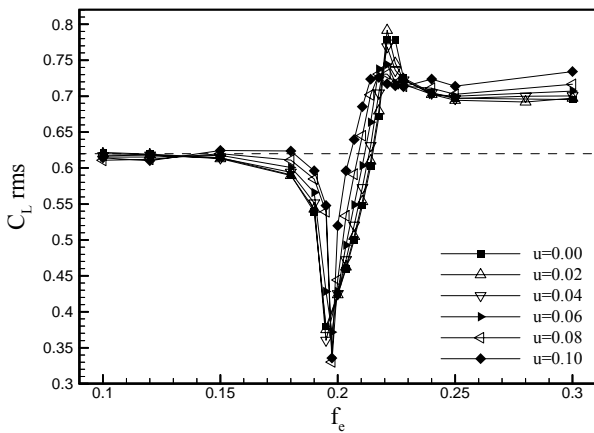


Figure 6: rms lift coefficient versus oscillation frequency.

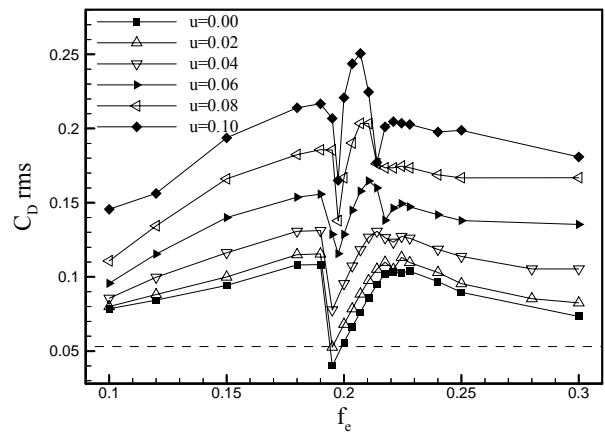


Figure 8: rms drag coefficient versus oscillation frequency.

For frequencies lower or higher than the natural frequency and throughout the lock-in bandwidth, the mean C_L is positive and all the more large since the ellipticity increases. The *rms* lift is similar or slightly lower than the natural lift fluctuation for oscillation frequencies lower than the lock-in band frequencies, but, for higher frequencies, *rms* lift presents values around 10% larger than the reference value. When lock-in occurs, a large jump is observed in mean and *rms* lift variation.

Figures 7 and 8 show the mean and *rms* drag coefficients versus the oscillation frequency. For frequencies lower or higher than the natural frequency, throughout the lock-in bandwidth, the mean C_D is similar to the natural one. A large jump occurs for lock-in frequencies with minimum and maximum values of mean drag around $\pm 9\%$ the natural reference value. The *rms* drag coefficient is globally greater than the natural value, all the more large since the ellipticity increases. Under lock-in conditions, variation of fluctuating drag coefficient depends on the ellipticity.

Figure 9 shows details of mean and fluctuating forces under lock-in conditions. Behaviors are different for each fundamental quantity. If Strouhal number variations are linear for all ellipticity values, it is not the case of the other quantities.

The beginning of the lock-in is characterized by a type of crisis, called here "lock-in crisis": a sudden jump can be observed in C_D mean, C_D and C_L rms at all ellipticity values defining the lowest and highest lock-in frequency, called f_e^L and f_e^H respectively. For C_D mean and C_L rms, minimum and maximum values are reached for the lowest and highest lock-in frequency respectively. These fundamental quantities increase with oscillation frequency, i.e. the slope of curves is positive. For example, curve of C_L rms is positive, but for small ellipticity $E=0.0$, 0.2 and 0.4 C_L rms always increases, whereas it converges to a maximum value for $E=0.8$ and 1.0 . Shape of C_D mean is rather different: for $E=0.0$, quasi-linear variation with oscillation frequency is observed whereas the C_D mean variation tends to a curvilinear pattern all the

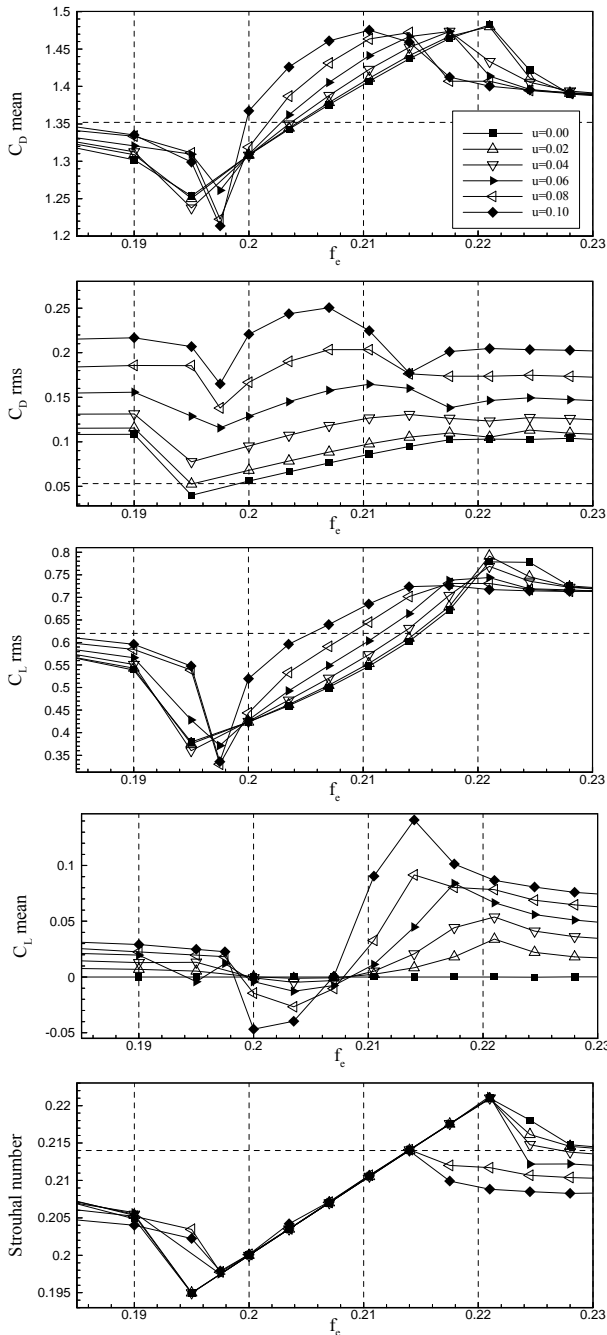


Figure 8: Details in the lock-in zone.

more the ellipticity increases, except for circular orbit. In this case, maximum value is reached before f_e^H and slope of the curve is negative for the highest lock-in frequency. Fluctuating drag coefficient presents a similar behavior comparing with mean C_D . For transversal motion, when ellipticity $E=0.0$, $C_D rms$ shows a linear variation with oscillation frequency, and maximum fluctuation is reached near f_e^H . However, slope and pattern of curves are widely modified with increasing ellipticity: variation of $C_D rms$ is all the less linear since the ellipticity increases. The maximum value is not

reached for the highest frequency, like C_D mean and $C_L rms$, but for a lower frequency than f_e^H , all the more lower since the ellipticity increases. Interestingly, the initial slope of curves C_D mean and $C_D rms$ are roughly identical (not show here).

Mean C_L coefficient presents an unexpected behavior under lock-in conditions. Mean C_L is equal to zero for pure cross-flow motion but show positive values when ellipticity is not zero, even if ellipticity is small, except for the low lock-in frequencies. Mean lift is negative for oscillation frequencies lower than a critical oscillation frequency equals to 0.207-0.208 and positive for frequencies higher than this critical value. Thus, for this critical frequency, the mean lift coefficient is zero. The maximum value of mean lift coefficient is reached for the highest lock-in frequency. However, the minimum mean lift does not correspond to the lowest lock-in frequency, but to a frequency between f_e^L and the critical frequency. It can be seen that minimum mean lift decreases and maximum increases all the more the ellipticity increases. Interestingly, C_L mean is unchanged for frequencies slightly higher than the lowest lock-in frequency: for $E=0.8$, lock-in occurs from $f_e=0.1975$, but mean C_L is changed only from $f_e=0.2$, after lock-in begins.

4. CONCLUSION

Unsteady flow past a circular cylinder in elliptic motion at $Re=300$ is studied numerically, using a original fully coupled resolution method, developed by the author, where the continuity equation is solved in its original form. The cylinder motion is gradually transformed from a transverse to a circular motion, with intermediate elliptic orbits. The present numerical investigation shows that:

- the vortex-shedding frequency of the oscillating cylinder changes to the frequency of cylinder vibrations when lock-in occurs;
- lock-in band-width decreases when orbit ellipticity increases;
- large jumps occur at the beginning and at the end of the lock-in.

Under lock-in conditions:

- slope and shape of curves of mean C_D and $C_D rms$ coefficients is widely modified when ellipticity increases, from linear to fully curvilinear shape. However, the initial slopes of these curves are roughly identical.
- slope and shape of $C_L rms$ curve changes with ellipticity too;
- mean C_L shows negative and positive values for frequencies lower and higher, respectively, than a critical frequency, around 0.207-0.208. For this critical frequency, mean C_L is equal to zero for all ellipticity values. Negative and positive values are all the more large since the orbit

ellipticity increases.

So, increasing orbit ellipticity of a circular cylinder induces a global increase of fundamental quantities. However, it seems that maximum values of mean C_D and C_D and C_L rms tend to limit values. It is not the case of mean C_L that already increases with ellipticity. Initial slopes of C_D mean and C_D and C_L rms, for lowest lock-in frequencies, are all the more large since negative mean C_L decreases, when orbit ellipticity increases. However maximum values of these coefficients seem all the more limited since positive mean C_L is large, when orbit ellipticity increases.

Other numerical simulations must be carried out and a deeper investigation is needed to understand and connect these phenomenons.

5. REFERENCES

- Al-Mdallal, Q.M., Lawrence, K.P., Kocabiyik, S., 2007, Forced streamwise oscillations of a circular cylinder: locked-on modes and resulting fluid forces. *J. Fluids and Structures*, **23**:681-701.
- Baranyi, L., 2004, Numerical simulation of flow past a cylinder in orbital motion. *J. Computational and Applied Mechanics*. **5(2)**: 209-222.
- Baranyi, L., 2008, Numerical simulation of flow around an orbiting cylinder at different ellipticity values. *J. Fluids and Structures* (in press).
- Bearman, P.W., Downie, M.J., Graham, J.M., Obasaju, E.D., 1985, Forces on cylinders in viscous oscillatory flow at low Keulegan-Carpenter numbers. *J. Fluid Mechanics*, **154**: 337-356.
- Chen, M.M., Dalton, C., Zhuang, L.X., 1995, Force on a circular cylinder in an elliptical orbital flow at low Keulegan-Carpenter numbers. *J. Fluids and Structures*, **9**: 617-638.
- Didier, E., and Borges, A.R.J., 2003, Unsteady Navier-Stokes equations: A fully coupled method for unstructured mesh. In Proc. *Conference on Modelling Fluid Flow*, 814-821. Budapest, Hungary.
- Didier, E., and Borges, A.R.J., 2005, Numerical simulation of two-dimensional cross-flow past a cylinder using an unstructured mesh based fully implicit second order coupled method. In Proc. *4th European & African Conference on Wind Engineering*. Praha.
- Didier, E., 2007, Flow simulation over two circular cylinders in tandem. *Comptes Rendus Mécanique*, **335**: 696-701.
- Didier, E., and Borges, A.R.J., 2007, Numerical predictions of low Reynolds number flow over an oscillating circular cylinder. *J. Computational and Applied Mechanics*. **8(1)**: 39-55.
- Didier, E., 2008, Convergência assintótica das quantidades fundamentais na modelação numérica do escoamento em torno de um cilindro circular. In Proc. *II Conf. Nacional de Métodos Numéricos em Mecânica de Fluidos e Termodinâmica*. Portugal.
- Griffin, O.M., Ramberg, S.E., 1975, Vortex shedding from a cylinder vibrating in line with an incident uniform flow. *J. Fluid Mech.*, **75**: 257-271.
- Koopmann, G.H., 1967, The vortex wakes of vibrating cylinders at low Reynolds numbers. *J. Fluid Mech.*, **28**: 501-512.
- Lewis, R.I., 2006, Application of the vortex cloud flow modelling to cylinders in orbital motion at low Reynolds numbers and comparisons with some published grid-based CFD predictions. In Proc. of *Conference on Modelling Fluid Flow*, 157-164. Budapest, Hungary.
- Meneghini, J.R., Bearman, P.W., 1995, Numerical simulation of high amplitude oscillatory flow about a circular cylinder. *J. Fluids and Structures*, **9**: 435-455.
- Mittal, S., and Kumar, V., 1999, Finite element study of vortex-induced cross-flow and in-line oscillations of a circular cylinder at low Reynolds numbers. *Int J Numer Meth Fluids*, **31**: 1087-1120.
- Nobari, M.R.H. and Naderan, H., 2006, A numerical study of flow past a cylinder with cross flow and inline oscillation. *Computers Fluids*, **35**: 393-415.
- Stansby, P.K., Rainey, R.C.T., 2001, on the orbital response of a rotating cylinder in a current. *J. Fluid Mechanics*, **439**: 87-108.
- Williamson, C.H.K., Roshko, A., 1988, Vortex formation in the wake of an oscillating cylinder. *J. Fluids and Structures*, **2**: 355-381.
- Williamson, C.H.K., Hess, P., Peter, M., Govardhan, R., 1998, Fluid loading and vortex dynamics for a body in elliptic orbits. In Proc. *Conference on Bluff Body Wakes and Vortex-Induced Vibration*. Washington, DC, USA.